Observation of an Excited Charm Baryon Ω_c^* Decaying to $\Omega_c^0\gamma$

B. Aubert,[1] M. Bona,[1] D. Boutigny,[1] F. Couderc,[1] Y. Karyotakis,[1] J. P. Lees,[1] V. Poireau,[1] V. Tisserand,[1] A. Zghiche,[1] E. Grauges,[2] A. Palano,[3] J. C. Chen,[4] N. D. Qi,[4] G. Rong,[4] P. Wang,[4] Y. S. Zhu,[4] G. Eigen,[5] I. Ofte,[5] B. Stugu,[5] G. S. Abrams,[6] M. Battaglia,[6] D. N. Brown,[6] J. Button-Shafer,[6] R. N. Cahn,[6] E. Charles,[6] M. S. Gill,[6] Y. Groysman,[6] R. G. Jacobsen,[6] J. A. Kadyk,[6] L. T. Kerth,[6] Yu. G. Kolomensky,[6] G. Kukartsev,[6] G. Lynch,[6] L. M. Mir,[6] T. J. Orimoto,[6] M. Pripstein,[6] N. A. Roe,[6] M. T. Ronan,[6] W. A. Wenzel,[6] P. del Amo Sanchez,[7] M. Barrett,[7] K. E. Ford,[7] A. J. Hart,[7] T. J. Harrison,[7] C. M. Hawkes,[7] A. T. Watson,[7] T. Held,[8] H. Koch,[8] B. Lewandowski,[8] M. Pelizaeus,[8] K. Peters,[8] T. Schroeder,[8] M. Steinke,[8] J. T. Boyd,[9] J. P. Burke,[9] W. N. Cottingham,[9] D. Walker,[9] D. J. Asgeirsson,[10] T. Cuhadar-Donszelmann,[10] B. G. Fulsom,[10] C. Hearty,[10] N. S. Knecht,[10] T. S. Mattison,[10] J. A. McKenna,[10] A. Khan,[11] P. Kyberd,[11] M. Saleem,[11] D. J. Sherwood,[11] L. Teodorescu,[11] V. E. Blinov,[12] A. D. Bukin,[12] V. P. Druzhinin,[12] V. B. Golubev,[12] A. P. Onuchin,[12] S. I. Serednyakov,[12] Yu. I. Skovpen,[12] E. P. Solodov,[12] K. Yu. Todyshev,[12] M. Bondioli,[13] M. Bruinsma,[13] M. Chao,[13] S. Curry,[13] I. Eschrich,[13] D. Kirkby,[13] A. J. Lankford,[13] P. Lund,[13] M. Mandelkern,[13] R. K. Mommsen,[13] W. Roethel,[13] D. P. Stoker,[13] S. Abachi,[14] C. Buchanan,[14] S. D. Foulkes,[15] J. W. Gary,[15] O. Long,[15] B. C. Shen,[15] K. Wang,[15] L. Zhang,[15] H. K. Hadavand,[16] E. J. Hill,[16] H. P. Paar,[16] S. Rahatlou,[16] V. Sharma,[16] J. W. Berryhill,[17] C. Campagnari,[17] A. Cunha,[17] B. Dahmes,[17] T. M. Hong,[17] D. Kovalskyi,[17] J. D. Richman,[17] T. W. Beck,[18] A. M. Eisner,[18] C. J. Flacco,[18] C. A. Heusch,[18] J. Kroseberg,[18] W. S. Lockman,[18] G. Nesom,[18] T. Schalk,[18] B. A. Schumm,[18] A. Seiden,[18] P. Spradlin,[18] D. C. Williams,[18] M. G. Wilson,[18] J. Albert,[19] E. Chen,[19] A. Dvoretskii,[19] F. Fang,[19] D. G. Hitlin,[19] I. Narsky,[19] T. Piatenko,[19] F. C. Porter,[19] A. Ryd,[19] G. Mancinelli,[20] B. T. Meadows,[20] K. Mishra,[20] M. D. Sokoloff,[20] F. Blanc,[21] P. C. Bloom,[21] S. Chen,[21] W. T. Ford,[21] J. F. Hirschauer,[21] A. Kreisel,[21] M. Nagel,[21] U. Nauenberg,[21] A. Olivas,[21] W. O. Ruddick,[21] J. G. Smith,[21] K. A. Ulmer,[21] S. R. Wagner,[21] J. Zhang,[21] A. Chen,[22] E. A. Eckhart,[22] A. Soffer,[22] W. H. Toki,[22] R. J. Wilson,[22] F. Winklmeier,[22] Q. Zeng,[22] D. D. Altenburg,[23] E. Feltresi,[23] A. Hauke,[23] H. Jasper,[23] J. Merkel,[23] A. Petzold,[23] B. Spaan,[23] T. Brandt,[24] V. Klose,[24] H. M. Lacker,[24] W. F. Mader,[24] R. Nogowski,[24] J. Schubert,[24] K. R. Schubert,[24] R. Schwierz,[24] J. E. Sundermann,[24] A. Volk,[24] D. Bernard,[25] G. R. Bonneaud,[25] E. Latour,[25] Ch. Thiebaux,[25] M. Verderi,[25] P. J. Clark,[26] W. Gradl,[26] F. Muheim,[26] S. Playfer,[26] A. I. Robertson,[26] Y. Xie,[26] M. Andreotti,[27] D. Bettoni,[27] C. Bozzi,[27] R. Calabrese,[27] G. Cibinetto,[27] E. Luppi,[27] M. Negrini,[27] A. Petrella,[27] L. Piemontese,[27] E. Prencipe,[27] F. Anulli,[28] R. Baldini-Ferroli,[28] A. Calcaterra,[28] R. de Sangro,[28] G. Finocchiaro,[28] S. Pacetti,[28] P. Patteri,[28] I. M. Peruzzi,[28,*] M. Piccolo,[28] M. Rama,[28] A. Zallo,[28] A. Buzzo,[29] R. Contri,[29] M. Lo Vetere,[29] M. M. Macri,[29] M. R. Monge,[29] S. Passaggio,[29] C. Patrignani,[29] E. Robutti,[29] A. Santroni,[29] S. Tosi,[29] G. Brandenburg,[30] K. S. Chaisanguanthum,[30] M. Morii,[30] J. Wu,[30] R. S. Dubitzky,[31] J. Marks,[31] S. Schenk,[31] U. Uwer,[31] W. Bhimji,[32] D. A. Bowerman,[32] P. D. Dauncey,[32] U. Egede,[32] R. L. Flack,[32] J. A. Nash,[32] M. B. Nikolich,[32] W. Panduro Vazquez,[32] D. J. Bard,[33] P. K. Behera,[33] X. Chai,[33] M. J. Charles,[33] U. Mallik,[33] N. T. Meyer,[33] V. Ziegler,[33] J. Cochran,[34] H. B. Crawley,[34] L. Dong,[34] V. Eyges,[34] W. T. Meyer,[34] S. Prell,[34] E. I. Rosenberg,[34] A. E. Rubin,[34] A. V. Gritsan,[35] A. G. Denig,[36] M. Fritsch,[36] G. Schott,[36] N. Arnaud,[37] M. Davier,[37] G. Grosdidier,[37] A. Höcker,[37] F. Le Diberder,[37] V. Lepeltier,[37] A. M. Lutz,[37] A. Oyanguren,[37] S. Pruvot,[37] S. Rodier,[37] P. Roudeau,[37] M. H. Schune,[37] A. Stocchi,[37] W. F. Wang,[37] G. Wormser,[37] C. H. Cheng,[38] D. J. Lange,[38] D. M. Wright,[38] C. A. Chavez,[39] I. J. Forster,[39] J. R. Fry,[39] E. Gabathuler,[39] R. Gamet,[39] K. A. George,[39] D. E. Hutchcroft,[39] D. J. Payne,[39] K. C. Schofield,[39] C. Touramanis,[39] A. J. Bevan,[40] F. Di Lodovico,[40] W. Menges,[40] R. Sacco,[40] G. Cowan,[41] H. U. Flaecher,[41] D. A. Hopkins,[41] P. S. Jackson,[41] T. R. McMahon,[41] S. Ricciardi,[41] F. Salvatore,[41] A. C. Wren,[41] D. N. Brown,[42] C. L. Davis,[42] J. Allison,[43] N. R. Barlow,[43] R. J. Barlow,[43] Y. M. Chia,[43] C. L. Edgar,[43] G. D. Lafferty,[43] M. T. Naisbit,[43] J. C. Williams,[43] J. I. Yi,[43] C. Chen,[44] W. D. Hulsbergen,[44] A. Jawahery,[44] C. K. Lae,[44] D. A. Roberts,[44] G. Simi,[44] G. Blaylock,[45] C. Dallapiccola,[45] S. S. Hertzbach,[45] X. Li,[45] T. B. Moore,[45] S. Saremi,[45] H. Staengle,[45] R. Cowan,[46] G. Sciolla,[46] S. J. Sekula,[46] M. Spitznagel,[46] F. Taylor,[46] R. K. Yamamoto,[46] H. Kim,[47] S. E. Mclachlin,[47] P. M. Patel,[47] S. H. Robertson,[47] A. Lazzaro,[48] V. Lombardo,[48] F. Palombo,[48] J. M. Bauer,[49] L. Cremaldi,[49] V. Eschenburg,[49] R. Godang,[49] R. Kroeger,[49] D. A. Sanders,[49] D. J. Summers,[49] H. W. Zhao,[49] S. Brunet,[50] D. Côté,[50] M. Simard,[50] P. Taras,[50] F. B. Viaud,[50] H. Nicholson,[51] N. Cavallo,[52,†] G. De Nardo,[52] F. Fabozzi,[52,†] C. Gatto,[52] L. Lista,[52] D. Monorchio,[52] P. Paolucci,[52] D. Piccolo,[52] C. Sciacca,[52] M. A. Baak,[53] G. Raven,[53] H. L. Snoek,[53] C. P. Jessop,[54] J. M. LoSecco,[54] T. Allmendinger,[55] G. Benelli,[55] L. A. Corwin,[55] K. K. Gan,[55] K. Honscheid,[55] D. Hufnagel,[55] P. D. Jackson,[55] H. Kagan,[55] R. Kass,[55] A. M. Rahimi,[55] J. J. Regensburger,[55] R. Ter-Antonyan,[55] Q. K. Wong,[55] N. L. Blount,[56] J. Brau,[56] R. Frey,[56] O. Igonkina,[56] J. A. Kolb,[56] M. Lu,[56] R. Rahmat,[56] N. B. Sinev,[56] D. Strom,[56]

J. Strube,[56] E. Torrence,[56] A. Gaz,[57] M. Margoni,[57] M. Morandin,[57] A. Pompili,[57] M. Posocco,[57] M. Rotondo,[57] F. Simonetto,[57] R. Stroili,[57] C. Voci,[57] M. Benayoun,[58] H. Briand,[58] J. Chauveau,[58] P. David,[58] L. Del Buono,[58] Ch. de la Vaissière,[58] O. Hamon,[58] B. L. Hartfiel,[58] Ph. Leruste,[58] J. Malclès,[58] J. Ocariz,[58] L. Roos,[58] G. Therin,[58] L. Gladney,[59] M. Biasini,[60] R. Covarelli,[60] C. Angelini,[61] G. Batignani,[61] S. Bettarini,[61] F. Bucci,[61] G. Calderini,[61] M. Carpinelli,[61] R. Cenci,[61] F. Forti,[61] M. A. Giorgi,[61] A. Lusiani,[61] G. Marchiori,[61] M. A. Mazur,[61] M. Morganti,[61] N. Neri,[61] E. Paoloni,[61] G. Rizzo,[61] J. J. Walsh,[61] M. Haire,[62] D. Judd,[62] D. E. Wagoner,[62] J. Biesiada,[63] N. Danielson,[63] P. Elmer,[63] Y. P. Lau,[63] C. Lu,[63] J. Olsen,[63] A. J. S. Smith,[63] A. V. Telnov,[63] F. Bellini,[64] G. Cavoto,[64] A. D'Orazio,[64] D. del Re,[64] E. Di Marco,[64] R. Faccini,[64] F. Ferrarotto,[64] F. Ferroni,[64] M. Gaspero,[64] L. Li Gioi,[64] M. A. Mazzoni,[64] S. Morganti,[64] G. Piredda,[64] F. Polci,[64] F. Safai Tehrani,[64] C. Voena,[64] M. Ebert,[65] H. Schröder,[65] R. Waldi,[65] T. Adye,[66] N. De Groot,[66] B. Franek,[66] E. O. Olaiya,[66] F. F. Wilson,[66] R. Aleksan,[67] S. Emery,[67] A. Gaidot,[67] S. F. Ganzhur,[67] G. Hamel de Monchenault,[67] W. Kozanecki,[67] M. Legendre,[67] G. Vasseur,[67] Ch. Yèche,[67] M. Zito,[67] X. R. Chen,[68] H. Liu,[68] W. Park,[68] M. V. Purohit,[68] J. R. Wilson,[68] M. T. Allen,[69] D. Aston,[69] R. Bartoldus,[69] P. Bechtle,[69] N. Berger,[69] R. Claus,[69] J. P. Coleman,[69] M. R. Convery,[69] M. Cristinziani,[69] J. C. Dingfelder,[69] J. Dorfan,[69] G. P. Dubois-Felsmann,[69] D. Dujmic,[69] W. Dunwoodie,[69] R. C. Field,[69] T. Glanzman,[69] S. J. Gowdy,[69] M. T. Graham,[69] P. Grenier,[69] V. Halyo,[69] C. Hast,[69] T. Hryn'ova,[69] W. R. Innes,[69] M. H. Kelsey,[69] P. Kim,[69] D. W. G. S. Leith,[69] S. Li,[69] S. Luitz,[69] V. Luth,[69] H. L. Lynch,[69] D. B. MacFarlane,[69] H. Marsiske,[69] R. Messner,[69] D. R. Muller,[69] C. P. O'Grady,[69] V. E. Ozcan,[69] A. Perazzo,[69] M. Perl,[69] T. Pulliam,[69] B. N. Ratcliff,[69] A. Roodman,[69] A. A. Salnikov,[69] R. H. Schindler,[69] J. Schwiening,[69] A. Snyder,[69] J. Stelzer,[69] D. Su,[69] M. K. Sullivan,[69] K. Suzuki,[69] S. K. Swain,[69] J. M. Thompson,[69] J. Va'vra,[69] N. van Bakel,[69] M. Weaver,[69] A. J. R. Weinstein,[69] W. J. Wisniewski,[69] M. Wittgen,[69] D. H. Wright,[69] A. K. Yarritu,[69] K. Yi,[69] C. C. Young,[69] P. R. Burchat,[70] A. J. Edwards,[70] S. A. Majewski,[70] B. A. Petersen,[70] C. Roat,[70] L. Wilden,[70] S. Ahmed,[71] M. S. Alam,[71] R. Bula,[71] J. A. Ernst,[71] V. Jain,[71] B. Pan,[71] M. A. Saeed,[71] F. R. Wappler,[71] S. B. Zain,[71] W. Bugg,[72] M. Krishnamurthy,[72] S. M. Spanier,[72] R. Eckmann,[73] J. L. Ritchie,[73] A. Satpathy,[73] C. J. Schilling,[73] R. F. Schwitters,[73] J. M. Izen,[74] X. C. Lou,[74] S. Ye,[74] F. Bianchi,[75] F. Gallo,[75] D. Gamba,[75] M. Bomben,[76] L. Bosisio,[76] C. Cartaro,[76] F. Cossutti,[76] G. Della Ricca,[76] S. Dittongo,[76] L. Lanceri,[76] L. Vitale,[76] V. Azzolini,[77] N. Lopez-March,[77] F. Martinez-Vidal,[77] Sw. Banerjee,[78] B. Bhuyan,[78] C. M. Brown,[78] D. Fortin,[78] K. Hamano,[78] R. Kowalewski,[78] I. M. Nugent,[78] J. M. Roney,[78] R. J. Sobie,[78] J. J. Back,[79] P. F. Harrison,[79] T. E. Latham,[79] G. B. Mohanty,[79] M. Pappagallo,[79] H. R. Band,[80] X. Chen,[80] B. Cheng,[80] S. Dasu,[80] M. Datta,[80] K. T. Flood,[80] J. J. Hollar,[80] P. E. Kutter,[80] B. Mellado,[80] A. Mihalyi,[80] Y. Pan,[80] M. Pierini,[80] R. Prepost,[80] S. L. Wu,[80] Z. Yu,[80] and H. Neal[81]

(*BABAR* Collaboration)

[1]*Laboratoire de Physique des Particules, IN2P3/CNRS et Université de Savoie, F-74941 Annecy-Le-Vieux, France*
[2]*Facultat de Fisica, Departament ECM, Universitat de Barcelona, E-08028 Barcelona, Spain*
[3]*Dipartimento di Fisica and INFN, Università di Bari, I-70126 Bari, Italy*
[4]*Institute of High Energy Physics, Beijing 100039, China*
[5]*Institute of Physics, University of Bergen, N-5007 Bergen, Norway*
[6]*Lawrence Berkeley National Laboratory and University of California, Berkeley, California 94720, USA*
[7]*University of Birmingham, Birmingham, B15 2TT, United Kingdom*
[8]*Institut für Experimentalphysik 1, Ruhr Universität Bochum, D-44780 Bochum, Germany*
[9]*University of Bristol, Bristol BS8 1TL, United Kingdom*
[10]*University of British Columbia, Vancouver, British Columbia, Canada V6T 1Z1*
[11]*Brunel University, Uxbridge, Middlesex UB8 3PH, United Kingdom*
[12]*Budker Institute of Nuclear Physics, Novosibirsk 630090, Russia*
[13]*University of California at Irvine, Irvine, California 92697, USA*
[14]*University of California at Los Angeles, Los Angeles, California 90024, USA*
[15]*University of California at Riverside, Riverside, California 92521, USA*
[16]*University of California at San Diego, La Jolla, California 92093, USA*
[17]*University of California at Santa Barbara, Santa Barbara, California 93106, USA*
[18]*Institute for Particle Physics, University of California at Santa Cruz, Santa Cruz, California 95064, USA*
[19]*California Institute of Technology, Pasadena, California 91125, USA*
[20]*University of Cincinnati, Cincinnati, Ohio 45221, USA*
[21]*University of Colorado, Boulder, Colorado 80309, USA*
[22]*Colorado State University, Fort Collins, Colorado 80523, USA*
[23]*Institut für Physik, Universität Dortmund, D-44221 Dortmund, Germany*
[24]*Institut für Kern- und Teilchenphysik, Technische Universität Dresden, D-01062 Dresden, Germany*

[25]Laboratoire Leprince-Ringuet, CNRS/IN2P3, Ecole Polytechnique, F-91128 Palaiseau, France
[26]University of Edinburgh, Edinburgh EH9 3JZ, United Kingdom
[27]Dipartimento di Fisica and INFN, Università di Ferrara, I-44100 Ferrara, Italy
[28]Laboratori Nazionali di Frascati dell'INFN, I-00044 Frascati, Italy
[29]Dipartimento di Fisica and INFN, Università di Genova, I-16146 Genova, Italy
[30]Harvard University, Cambridge, Massachusetts 02138, USA
[31]Physikalisches Institut, Universität Heidelberg, Philosophenweg 12, D-69120 Heidelberg, Germany
[32]Imperial College London, London, SW7 2AZ, United Kingdom
[33]University of Iowa, Iowa City, Iowa 52242, USA
[34]Iowa State University, Ames, Iowa 50011-3160, USA
[35]Johns Hopkins University, Baltimore, Maryland 21218, USA
[36]Institut für Experimentelle Kernphysik, Universität Karlsruhe, D-76021 Karlsruhe, Germany
[37]Laboratoire de l'Accélérateur Linéaire, IN2P3/CNRS et Université Paris-Sud 11, Centre Scientifique d'Orsay, B.P. 34, F-91898 ORSAY Cedex, France
[38]Lawrence Livermore National Laboratory, Livermore, California 94550, USA
[39]University of Liverpool, Liverpool L69 7ZE, United Kingdom
[40]Queen Mary, University of London, E1 4NS, United Kingdom
[41]University of London, Royal Holloway, and Bedford New College, Egham, Surrey TW20 0EX, United Kingdom
[42]University of Louisville, Louisville, Kentucky 40292, USA
[43]University of Manchester, Manchester M13 9PL, United Kingdom
[44]University of Maryland, College Park, Maryland 20742, USA
[45]University of Massachusetts, Amherst, Massachusetts 01003, USA
[46]Laboratory for Nuclear Science, Massachusetts Institute of Technology, Cambridge, Massachusetts 02139, USA
[47]McGill University, Montréal, Québec, Canada H3A 2T8
[48]Dipartimento di Fisica and INFN, Università di Milano, I-20133 Milano, Italy
[49]University of Mississippi, University, Mississippi 38677, USA
[50]Physique des Particules, Université de Montréal, Montréal, Québec, Canada H3C 3J7
[51]Mount Holyoke College, South Hadley, Massachusetts 01075, USA
[52]Dipartimento di Scienze Fisiche and INFN, Università di Napoli Federico II, I-80126, Napoli, Italy
[53]NIKHEF, National Institute for Nuclear Physics and High Energy Physics, NL-1009 DB Amsterdam, The Netherlands
[54]University of Notre Dame, Notre Dame, Indiana 46556, USA
[55]Ohio State University, Columbus, Ohio 43210, USA
[56]University of Oregon, Eugene, Oregon 97403, USA
[57]Dipartimento di Fisica and INFN, Università di Padova, I-35131 Padova, Italy
[58]Laboratoire de Physique Nucléaire et de Hautes Energies, IN2P3/CNRS, Université Pierre et Marie Curie-Paris6, Université Denis Diderot-Paris7, F-75252 Paris, France
[59]University of Pennsylvania, Philadelphia, Pennsylvania 19104, USA
[60]Dipartimento di Fisica and INFN, Università di Perugia, I-06100 Perugia, Italy
[61]Dipartimento di Fisica, Scuola Normale Superiore, and INFN, Università di Pisa, I-56127 Pisa, Italy
[62]Prairie View A&M University, Prairie View, Texas 77446, USA
[63]Princeton University, Princeton, New Jersey 08544, USA
[64]Dipartimento di Fisica and INFN, Università di Roma La Sapienza, I-00185 Roma, Italy
[65]Universität Rostock, D-18051 Rostock, Germany
[66]Rutherford Appleton Laboratory, Chilton, Didcot, Oxon, OX11 0QX, United Kingdom
[67]DSM/Dapnia, CEA/Saclay, F-91191 Gif-sur-Yvette, France
[68]University of South Carolina, Columbia, South Carolina 29208, USA
[69]Stanford Linear Accelerator Center, Stanford, California 94309, USA
[70]Stanford University, Stanford, California 94305-4060, USA
[71]State University of New York, Albany, New York 12222, USA
[72]University of Tennessee, Knoxville, Tennessee 37996, USA
[73]University of Texas at Austin, Austin, Texas 78712, USA
[74]University of Texas at Dallas, Richardson, Texas 75083, USA
[75]Dipartimento di Fisica Sperimentale and INFN, Università di Torino, I-10125 Torino, Italy
[76]Dipartimento di Fisica and INFN, Università di Trieste, I-34127 Trieste, Italy
[77]IFIC, Universitat de Valencia-CSIC, E-46071 Valencia, Spain
[78]University of Victoria, Victoria, British Columbia, Canada V8W 3P6
[79]Department of Physics, University of Warwick, Coventry CV4 7AL, United Kingdom
[80]University of Wisconsin, Madison, Wisconsin 53706, USA
[81]Yale University, New Haven, Connecticut 06511, USA

(Received 25 August 2006; published 6 December 2006)

We report the first observation of an excited singly charmed baryon Ω_c^* (css) in the radiative decay $\Omega_c^0\gamma$, where the Ω_c^0 baryon is reconstructed in the decays to the final states $\Omega^-\pi^+$, $\Omega^-\pi^+\pi^0$, $\Omega^-\pi^+\pi^-\pi^+$, and $\Xi^-K^-\pi^+\pi^+$. This analysis is performed using a data set of 230.7 fb^{-1} collected by the *BABAR* detector at the PEP-II asymmetric-energy B factory at the Stanford Linear Accelerator Center. The mass difference between the Ω_c^* and the Ω_c^0 baryons is measured to be $70.8 \pm 1.0(\text{stat}) \pm 1.1(\text{syst})$ MeV$/c^2$. We also measure the ratio of inclusive production cross sections of Ω_c^* and Ω_c^0 in e^+e^- annihilation.

DOI: 10.1103/PhysRevLett.97.232001 PACS numbers: 14.20.Lq, 13.30.Ce

The production of charm baryons is largely unexplored and provides an interesting environment to study the dynamics of quark-gluon interactions. All singly charmed baryons having zero orbital angular momentum have been discovered [1], except for the $J^P = \frac{3}{2}^+$ css state, denoted as Ω_c^*. A nonrelativistic QCD effective field theory calculation predicts the difference between the mass of Ω_c^* ($M_{\Omega_c^*}$) and the mass of Ω_c^0 ($M_{\Omega_c^0}$), ΔM, to be between 50 and 73 MeV$/c^2$ [2]. A lattice QCD calculation gives $\Delta M = 94 \pm 10$ MeV$/c^2$ [3]. New quadratic baryon mass relations predict a mass of $M_{\Omega_c^*} = 2767 \pm 7$ MeV$/c^2$ [4], and several other predictions for $M_{\Omega_c^*}$ exist around 2770 MeV$/c^2$ [5–11], implying $\Delta M = 70$–75 MeV$/c^2$.

Here we report the observation of an excited baryon Ω_c^* produced inclusively in $e^+e^- \to \Omega_c^* X$ processes, where X denotes the rest of the event. We measure the mass difference, ΔM, and the ratio of the production cross section of $e^+e^- \to \Omega_c^* X$ relative to $e^+e^- \to \Omega_c^0 X$. Throughout this Letter, for any given mode, the corresponding charge conjugate reaction is also implied.

The data used in this analysis were collected with the *BABAR* detector at the PEP-II asymmetric-energy e^+e^- storage rings. The data set corresponds to an integrated luminosity of 209.1 fb^{-1} collected at a center-of-mass (c.m.) energy of $\sqrt{s} = 10.58$ GeV, near the peak of the $\Upsilon(4S)$ resonance, and 21.6 fb^{-1} collected approximately 40 MeV below the $\Upsilon(4S)$ mass.

The *BABAR* detector is described elsewhere [12]. Charged tracks are reconstructed with a five-layer, double-sided silicon vertex tracker (SVT) and a 40-layer drift chamber (DCH) with a helium-based gas mixture, placed in a 1.5-T uniform magnetic field produced by a superconducting solenoidal magnet. Kaons, pions, and protons are identified using likelihood ratios calculated from the ionization energy loss (dE/dx) measurements in the SVT and DCH, and from the observed pattern of Cherenkov light in an internally reflecting ring imaging detector. Photons are identified as isolated electromagnetic showers in a CsI(Tl) electromagnetic calorimeter (EMC). Large samples of Monte Carlo (MC) simulated data are used for determination of signal detection efficiencies and for the optimization of the selection criteria. These are generated using JETSET [13] and the detector response is simulated with GEANT4 [14].

The Ω_c^* candidate is identified through its radiative decay, $\Omega_c^* \to \Omega_c^0\gamma$, where the Ω_c^0 is reconstructed exclusively in the following four decay modes, which are expected to provide the best signal-to-background ratio:

$$\Omega_c^0 \to \Omega^-\pi^+, \qquad \Omega^- \to \Lambda K^- \qquad \text{(O1)}$$

$$\Omega_c^0 \to \Omega^-\pi^+\pi^0, \qquad \Omega^- \to \Lambda K^- \qquad \text{(O2)}$$

$$\Omega_c^0 \to \Omega^-\pi^+\pi^-\pi^+, \qquad \Omega^- \to \Lambda K^- \qquad \text{(O3)}$$

$$\Omega_c^0 \to \Xi^-K^-\pi^+\pi^+, \qquad \Xi^- \to \Lambda\pi^-. \qquad \text{(C1)}$$

The labels in parentheses to the right of each decay mode designate the four final states of the Ω_c^0 decay.

A $\Lambda \to p\pi^-$ candidate is reconstructed by identifying a proton track, combining it with an oppositely charged track identified as a π^-, and fitting the tracks to a common vertex. Here and throughout this analysis, all reconstructed baryon candidates are required to have an acceptable χ^2 from the vertex fit. The flight distance of each Λ candidate between its decay vertex and that of its parent (Ω^- or Ξ^-) is required to be greater than 0.30 cm. The $\Lambda \to p\pi^-$ signal is fitted using a sum of two Gaussian functions with a common mean. The signal region is defined by $|M_{p\pi^-} - M_\Lambda| < 3.8$ MeV$/c^2$ ($\approx 2\sigma_{\text{rms}}$), where M_Λ is the fitted peak position of the Λ and σ_{rms} is defined by $\sigma_{\text{rms}}^2 \equiv f_1\sigma_1^2 + f_2\sigma_2^2$, where f_1 and f_2 are the fractions of the two Gaussian functions, and σ_1 and σ_2 are the two corresponding widths as obtained from the fit. The reconstructed Λ candidate is then combined with an identified K^- (π^-) to form an Ω^- (Ξ^-) candidate. The Λ and the K^- (π^-) tracks are fitted to a common vertex, and the flight distance of each Ω^- or Ξ^- candidate between its decay vertex and that of its parent (Ω_c^0) is required to be greater than 0.25 cm. Mass windows of $|M_{\Lambda K^-} - M_{\Omega^-}| < 5.2$ MeV$/c^2$($\approx 2\sigma_{\text{rms}}$) and $|M_{\Lambda\pi^-} - M_{\Xi^-}| < 6.0$ MeV$/c^2$($\approx 2\sigma_{\text{rms}}$) are used to select $\Omega^- \to \Lambda K^-$ and $\Xi^- \to \Lambda\pi^-$ candidates, respectively, where M_{Ω^-} and M_{Ξ^-} represent the fitted peak positions of Ω^- and Ξ^-.

For the decay mode (O2), the π^0 candidates are reconstructed by combining two photons. To enhance the π^0 signal over combinatorial background, we require photons to have a minimum energy of 80 MeV in the laboratory frame, to have a lateral shower shape consistent with that of a photon, and to be well separated from other tracks and clusters in the EMC. We require

$|M_{\gamma\gamma} - M_{\pi^0}| < 12.5\ \mathrm{MeV}/c^2 (2.5\sigma)$, where M_{π^0} is the fitted peak position of the invariant mass of the two photons.

For decays (O1)–(O3), the reconstructed Ω^- is combined with a (π^+, $\pi^+\pi^0$, $\pi^+\pi^-\pi^+$) to form an Ω_c^0, and fitted to a common vertex. For (C1), the reconstructed Ξ^- is combined with an identified K^- and two π^+ tracks and fitted to a common vertex. The invariant mass of reconstructed Ω_c^0 candidates is required to lie within $\pm 2.5\sigma_{\mathrm{rms}}$ of the central fitted value. The mass resolution is $\sigma_{\mathrm{rms}} \approx 6\ \mathrm{MeV}/c^2$ for (O1), (O3), and (C1), and $\sigma_{\mathrm{rms}} \approx 13\ \mathrm{MeV}/c^2$ for (O2). The resolution in (O2) is dominated by the measurement of the photon energies from the π^0 decay.

An Ω_c^* candidate is formed by combining a reconstructed Ω_c^0 with a photon, applying the same photon selection requirements listed above for photons from π^0 decay. For (O2), it is required that the photon is not one of the π^0 daughters.

Though eliminating most Ω_c^* baryons from B decays, the requirement that the scaled momentum of Ω_c^* candidates, ($x_p(\Omega_c^*)$), be greater than 0.5 significantly reduces combinatorial background from $e^+e^- \to q\bar{q}$ (where $q = u, d, s$). The scaled momentum is defined as $x_p = p^*/p^*_{\mathrm{max}}$, where p^* is the reconstructed momentum in the c.m. frame and $p^*_{\mathrm{max}} = \sqrt{s/4 - M^2}$, with M being the mass of the particle.

Figure 1 shows the reconstructed invariant mass distributions of Ω_c^0 candidates with $x_p(\Omega_c^0) > 0.5$. Clear peaks indicating production of Ω_c^0 are visible in each of the modes represented in Fig. 1. The invariant mass resolution is improved by 25% by using the variable $M_{\Omega^-\pi^+} - M_{\Omega^-} + M_{\Omega^-}^{\mathrm{PDG}}$, instead of $M_{\Omega^-\pi^+}$, where M_{Ω^-} is the reconstructed mass of the Ω^- and $M_{\Omega^-}^{\mathrm{PDG}}$ is the world average mass of the Ω^- [1]. An unbinned extended maximum likelihood (ML) fit is performed to extract the signal yield. For each mode, a double Gaussian function with a common mean is used to fit the signal and a first-order polynomial is used to model the combinatorial background. The mass resolution in each decay mode is obtained from a large sample of MC signal events reconstructed and processed in the same way as data. For the fits shown in Fig. 1, the widths of the signal line shapes are fixed to the values from MC simulation. The fit shown in Fig. 1(a) results in a raw (i.e., uncorrected) yield of $156 \pm 15(\mathrm{stat})$ events and a mean mass of $2693.3 \pm 0.6(\mathrm{stat})\ \mathrm{MeV}/c^2$. For the other three Ω_c^0 decay modes the mean masses are fixed at $2693.3\ \mathrm{MeV}/c^2$, and a second-order polynomial is used to model the combinatorial background. The fitted raw yields are $92^{+26}_{-25}(\mathrm{stat})$, $23^{+10}_{-9}(\mathrm{stat})$, and $34^{+15}_{-14}(\mathrm{stat})$ events for (O2), (O3), and (C1) decay modes, respectively.

For Ω_c^* candidate selection, we require $x_p(\Omega_c^*) > 0.5$ but make no direct cut on $x_p(\Omega_c^0)$. The invariant mass distributions of $\Omega_c^* \to \Omega_c^0\gamma$ candidates are shown in Fig. 2. The invariant mass resolution is improved by $\approx 40\%$ by using the variable $M_{\Omega_c^0\gamma} - M_{\Omega_c^0} + M_{\Omega_c^0}^{\mathrm{PDG}}$, instead of $M_{\Omega_c^0\gamma}$,

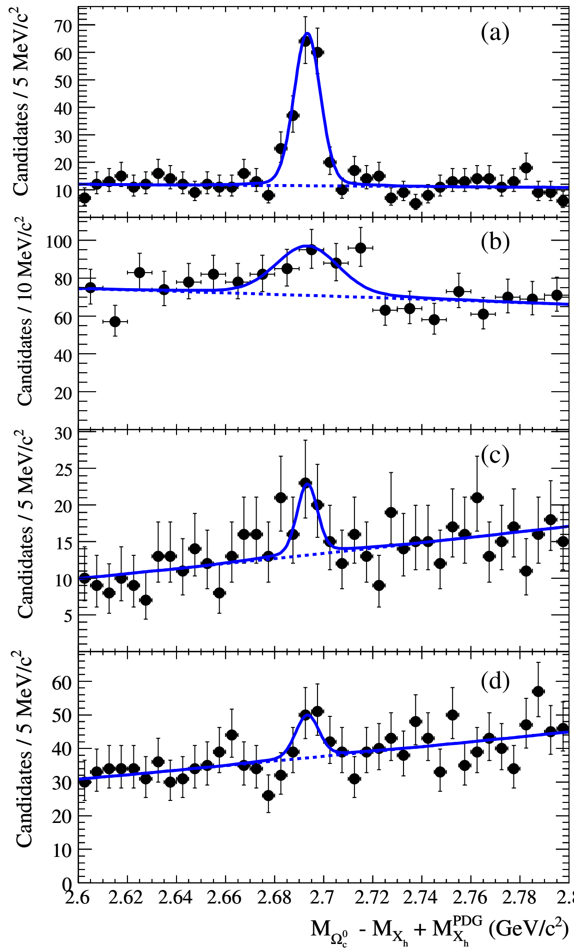

FIG. 1 (color online). The invariant mass distributions of Ω_c^0 candidates reconstructed in the Ω_c^0 decay modes into (a) $\Omega^-\pi^+$, (b) $\Omega^-\pi^+\pi^0$, (c) $\Omega^-\pi^+\pi^-\pi^+$, and (d) $\Xi^-K^-\pi^+\pi^+$. For all of these, we require $x_p(\Omega_c^0) > 0.5$. Here $M_{\Omega_c^0}$ is the reconstructed mass of the Ω_c^0 candidates, and X_h denotes the daughter hyperon. The points with error bars represent the data, the dashed line represents the combinatorial background, and the solid line the sum of signal and background.

where $M_{\Omega_c^0}$ is the reconstructed mass of the Ω_c^0 and $M_{\Omega_c^0}^{\mathrm{PDG}}$ is the world average mass of the Ω_c^0 ($2697.5\ \mathrm{MeV}/c^2$) [1]. A clear peak from $\Omega_c^* \to \Omega_c^0\gamma$ ($\Omega_c^0 \to \Omega^-\pi^+$) production can be seen in Fig. 2(a). The scaled Ω_c^0 sidebands, which are also shown in Fig. 2, show no peak in the mass distribution. The distribution is fitted with the Crystal Ball function [15] to model the signal and the product of a fourth-order polynomial and a two-body phase space function [1] to model the combinatorial background. The signal shape parameters are fixed to the values found from MC simulation except for the mean of the distribution. The invariant mass resolution is $4.0\ \mathrm{MeV}/c^2$. The fit results in $\Delta M = 69.9 \pm 1.4(\mathrm{stat})\ \mathrm{MeV}/c^2$ and a raw yield of $39^{+10}_{-9}(\mathrm{stat})$ events. The fit is superimposed on Fig. 2(a). The signal observed for $\Omega_c^* \to \Omega_c^0\gamma$ ($\Omega_c^0 \to \Omega^-\pi^+$) corresponds to a signifi-

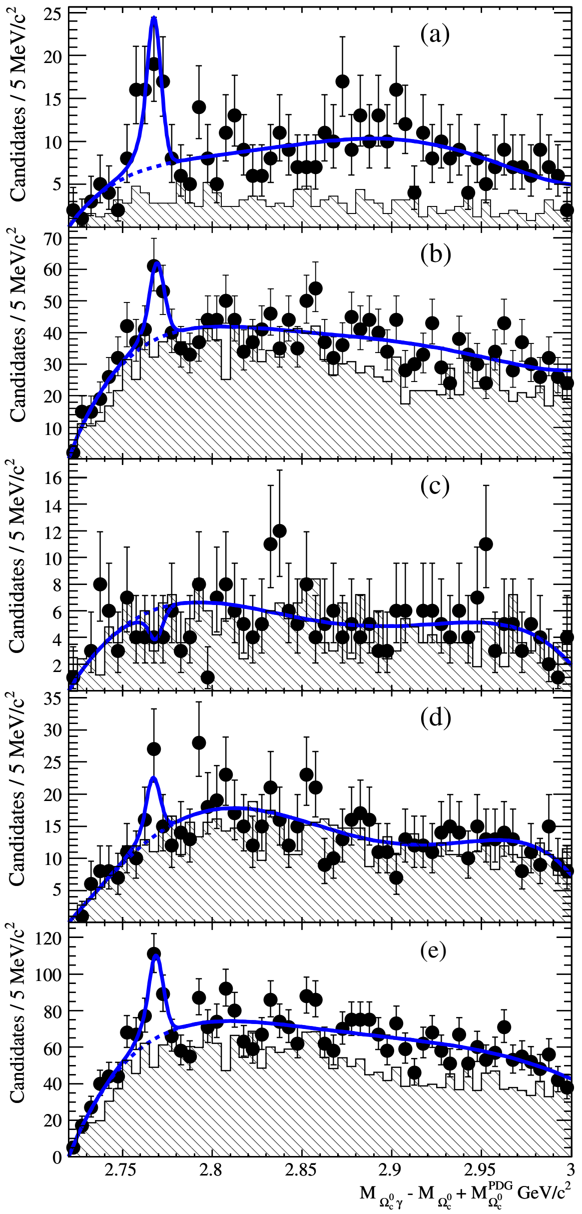

FIG. 2 (color online). The invariant mass distributions of $\Omega_c^* \to \Omega_c^0\gamma$ candidates, with Ω_c^0 reconstructed in the decay modes (a) $\Omega^-\pi^+$, (b) $\Omega^-\pi^+\pi^0$, (c) $\Omega^-\pi^+\pi^-\pi^+$, (d) $\Xi^-K^-\pi^+\pi^+$, and (e) for the combined decay modes [(O1)–(O3) and (C1)]. For all of these, we require $x_p(\Omega_c^*) > 0.5$. Here $M_{\Omega_c^0}\gamma$ is the reconstructed mass of the Ω_c^* candidates, and $M_{\Omega_c^0}$ is the reconstructed mass of the Ω_c^0. The points with error bars represent the data, the dashed line represents the combinatorial background, and the solid line the sum of signal and background. The shaded histograms represent the mass distribution expected from the mass sideband of Ω_c^0.

cance of 4.2 standard deviations (σ) including the systematic uncertainty on the observed yield. The significance is derived from $\sqrt{2\ln(L_{\max}/L_0)}$, where $L_{\max}$ and L_0 are the likelihoods for fits with and without a resonance peak component, respectively. The systematic uncertainty is discussed later. We use a similar fit procedure for (O2), (O3), and (C1) decay modes to extract the signal yields. For (O3), $M_{\Omega_c^0}$ is fixed to the value obtained from the process (O1). The fits result in raw yields of 55^{+16}_{-15}(stat), -5 ± 5(stat), and 20 ± 9(stat) events for (O2), (O3), and (C1), respectively.

For all decay modes we determine the ratio of inclusive production cross sections,

$$R = \frac{\sigma(e^+e^- \to \Omega_c^* X, x_p(\Omega_c^*) > 0.5)}{\sigma(e^+e^- \to \Omega_c^0 X, x_p(\Omega_c^0) > 0.5)},$$

where the scaled momentum of the Ω_c^* (Ω_c^0) is required to be greater than 0.5 in the numerator (denominator) cross section. We assume that $\mathcal{B}(\Omega_c^* \to \Omega_c^0\gamma) = 100\%$, and include Ω_c^0 baryons coming from Ω_c^* decay as part of the denominator cross section, provided they satisfy the $x_p(\Omega_c^0)$ requirement. The relative detection efficiencies ($\epsilon_{\Omega_c^*}/\epsilon_{\Omega_c^0}$) of the Ω_c^* compared to Ω_c^0 within these momentum ranges are estimated from MC simulation and are listed in Table I, along with the results for the cross section ratios R.

We combine (O1)–(O3) and (C1) and perform a single ML fit. The fit results in $\Delta M = 70.8 \pm 1.0(\mathrm{stat})\ \mathrm{MeV}/c^2$, a raw signal yield of 105 ± 21(stat) events, with a significance of 5.2σ (including systematic uncertainty), and a ratio $R = 1.01 \pm 0.23$(stat). This procedure weights the individual decay modes by the observed number of Ω_c^0 baryons in the data, and results in the minimum overall error on the combined value of R. The results are summarized in Table I.

Several sources of systematic uncertainty in the fitted signal yields are considered. The largest uncertainties arise from the fits to the mass spectra. These are estimated by repeating the fits, varying the fixed parameters of the fitted signal functions by ± 1 standard deviation, and varying the functional parametrization of the background. The systematic uncertainty on the yield from the combined Ω_c^* modes is 6%. The systematic uncertainty on ΔM is dominated by the photon energy scale and is 1.5%. This is estimated from the distribution of reconstructed masses of low-energy neutral pions. The uncertainty in the fitting procedure leads to a systematic uncertainty of 11% on the ratio R, measured from the combined modes. There are also systematic uncertainties of 1.8% from the photon reconstruction efficiency, and 1.4% due to the limited MC sample size. The uncertainties from tracking, particle identification, selection of intermediate hyperon candidates, daughter branching fractions [1], and luminosity approximately cancel in the ratio, since the Ω_c^* analysis uses the same selection and data sample as the Ω_c^0 analysis. The sensitivity to fragmentation modeling is negligible. A possible additional uncertainty arises from multiple candidates found in ≈10% of the events in the data, usually due to a common hyperon combined with alternative particles from the rest of the

TABLE I. The mass difference, $\Delta M = M_{\Omega_c^*} - M_{\Omega_c^0}$ (MeV/c^2), the fitted signal yield, Y (events), the Ω_c^* signal significance, S (in σ), the relative detection efficiency, $\epsilon_{\Omega_c^*}/\epsilon_{\Omega_c^0}$, and the ratio of inclusive production cross sections, R, as defined in the text. The first uncertainty is statistical, and the second is systematic.

Decay mode	ΔM (MeV/c^2)	Y (events)	S (σ)	$\epsilon_{\Omega_c^*}/\epsilon_{\Omega_c^0}$	R
(O1)	$69.9 \pm 1.4 \pm 1.0$	$39^{+10}_{-9} \pm 6$	4.2	0.35	$0.71^{+0.19}_{-0.18} \pm 0.11$
(O2)	$71.8 \pm 1.3 \pm 1.1$	$55^{+16}_{-15} \pm 6$	3.4	0.34	$1.76^{+0.71}_{-0.69} \pm 0.21$
(O3)	69.9 (fixed)	$-5 \pm 5 \pm 1$	$\cdots$	0.33	$-0.66^{+0.74}_{-0.66} \pm 0.13$
(C1)	$69.4^{+1.9}_{-2.0} \pm 1.0$	$20 \pm 9 \pm 3$	2.0	0.35	$1.70^{+1.02}_{-1.00} \pm 0.34$
Combined	$70.8 \pm 1.0 \pm 1.1$	$105 \pm 21 \pm 6$	5.2	0.34	$1.01 \pm 0.23 \pm 0.11$

event to form Ω_c^* candidates. These are uniformly distributed in $M_{\Omega_c^*}$ and are hence absorbed into the background parametrization, with no evidence for multiple candidates peaking in mass.

In summary, we report the first observation of an excited singly charmed baryon Ω_c^* (css) decaying to Ω_c^0 and a photon, with a significance of 5.2σ, and measure the mass difference between Ω_c^* and Ω_c^0 to be $\Delta M = 70.8 \pm 1.0(\text{stat}) \pm 1.1(\text{syst})$ MeV/c^2. This is consistent with the theoretical prediction in [2,4–11] and below that described in [3]. We also measure the ratio of inclusive production cross sections, $R = 1.01 \pm 0.23(\text{stat}) \pm 0.11(\text{syst})$.

We are grateful for the excellent luminosity and machine conditions provided by our PEP-II colleagues, and for the substantial dedicated effort from the computing organizations that support *BABAR*. The collaborating institutions wish to thank SLAC for its support and kind hospitality. This work is supported by DOE and NSF (USA), NSERC (Canada), IHEP (China), CEA and CNRS-IN2P3 (France), BMBF and DFG (Germany), INFN (Italy), FOM (The Netherlands), NFR (Norway), MIST (Russia), and PPARC (United Kingdom). Individuals have received support from the Marie Curie EIF (European Union) and the A. P. Sloan Foundation.

*Also with Dipartimento di Fisica, Università di Perugia, Perugia, Italy.

†Also with Università della Basilicata, Potenza, Italy.

[1] S. Eidelman *et al.*, Phys. Lett. B **592**, 1 (2004).

[2] N. Mathur *et al.*, Phys. Rev. D **66**, 014502 (2002).

[3] R. M. Woloshyn, Nucl. Phys. B, Proc. Suppl. **93**, 38 (2001).

[4] L. Burakovsky, T. Goldman, and L. P. Horwitz, Phys. Rev. D **56**, 7124 (1997).

[5] M. J. Savage, Phys. Lett. B **359**, 189 (1995).

[6] J. L. Rosner, Phys. Rev. D **52**, 6461 (1995).

[7] R. Roncaglia *et al.*, Phys. Rev. D **52**, 1722 (1995).

[8] D. B. Lichtenberg *et al.*, Phys. Rev. D **53**, 6678 (1996).

[9] A. Zalewska and K. Zalewski, hep-ph/9608240.

[10] L. Ya. Glozman and D. O. Riska, Nucl. Phys. **A603**, 326 (1996).

[11] E. Jenkins, Phys. Rev. D **54**, 4515 (1996).

[12] B. Aubert *et al.* (*BABAR* Collaboration), Nucl. Instrum. Methods Phys. Res., Sect. A **479**, 1 (2002).

[13] T. Sjöstrand, Comput. Phys. Commun. **82**, 74 (1994).

[14] S. Agostinelli *et al.* (GEANT4 Collaboration), Nucl. Instrum. Methods Phys. Res., Sect. A **506**, 250 (2003).

[15] $\text{CB} = e^{-\alpha^2/2}(n/|\alpha|)^n(n/|\alpha| - |\alpha| - y)$ for $y < \alpha$, $\text{CB} = e^{-\alpha^2/2}$ for $y > \alpha$; D. Antreasyan *et al.* (Crystal Ball Collaboration), Crystal Ball Note, 1983, p. 321.